ACCEPTED BY THE ASTROPHYSICAL JOURNAL
Preprint typeset using LaTeX style emulateapj v. 10/09/06

POSSIBLE RESONANCES IN THE ^{12}C + ^{12}C FUSION RATE AND SUPERBURST IGNITION

RANDALL L. COOPER
Kavli Institute for Theoretical Physics, University of California, Santa Barbara, CA 93106

ANDREW W. STEINER AND EDWARD F. BROWN
Department of Physics & Astronomy, National Superconducting Cyclotron Laboratory, and the Joint Institute for Nuclear Astrophysics, Michigan State University, East Lansing, MI

Accepted by THE ASTROPHYSICAL JOURNAL

ABSTRACT

Observationally inferred superburst ignition depths are shallower than models predict. We address this discrepancy by reexamining the superburst trigger mechanism. We first explore the hypothesis of Kuulkers et al. that exothermic electron captures trigger superbursts. We find that all electron capture reactions are thermally stable in accreting neutron star oceans and thus are not a viable trigger mechanism. Fusion reactions other than ^{12}C + ^{12}C are infeasible as well since the possible reactants either deplete at much shallower depths or have prohibitively large Coulomb barriers. Thus we confirm the proposal of Cumming & Bildsten and Strohmayer & Brown that ^{12}C + ^{12}C triggers superbursts. We then examine the ^{12}C + ^{12}C fusion rate. The reaction cross-section is experimentally unknown at astrophysically relevant energies, but resonances exist in the ^{12}C + ^{12}C system throughout the entire measured energy range. Thus it is likely, and in fact has been predicted, that a resonance exists near the Gamow peak energy $E^{\rm pk} \approx 1.5$ MeV. For such a hypothetical 1.5 MeV resonance, we derive both a fiducial value and upper limit to the resonance strength $(\omega\gamma)_{\rm R}$ and find that such a resonance could decrease the theoretically predicted superburst ignition depth by up to a factor of 4; in this case, observationally inferred superburst ignition depths would accord with model predictions for a range of plausible neutron star parameters. Said differently, such a resonance would decrease the temperature required for unstable ^{12}C ignition at a column depth 10^{12} g cm^{-2} from 6×10^8 K to 5×10^8 K. A resonance at 1.5 MeV would not strongly affect the ignition density of Type Ia supernovae, but it would lower the temperature at which ^{12}C ignites in massive post–main-sequence stars. Determining the existence of a strong resonance in the Gamow window requires measurements of the ^{12}C + ^{12}C cross-section down to a center-of-mass energy near 1.5 MeV, which is within reach of the proposed DUSEL facility.

Subject headings: nuclear reactions, nucleosynthesis, abundances — stars: neutron — X-rays: bursts

1. INTRODUCTION

Superbursts are long, energetic, and rare thermonuclear flashes on accreting neutron stars in low-mass X-ray binaries. Their durations ($\sim$ hours), fluences ($\sim 10^{42}$ ergs), and recurrence times ($\sim$ years) distinguish superbursts from their typical hydrogen- and helium-triggered counterparts (for reviews, see Kuulkers 2004; Cumming 2005; Strohmayer & Bildsten 2006). As of this writing, astronomers have detected 15 superbursts from 10 sources (Kuulkers 2004; in't Zand et al. 2004; Remillard et al. 2005; Kuulkers 2005; Keek et al. 2008, and references therein).

The proposal (Cumming & Bildsten 2001; Strohmayer & Brown 2002) that thermally unstable ^{12}C fusion (Woosley & Taam 1976; Taam & Picklum 1978; Brown & Bildsten 1998) triggers superbursts offers a reasonable explanation of their origin. Cooling model fits to superburst light curves (Cumming & Macbeth 2004; Cumming et al. 2006) as well as observed fluences and recurrence times (e.g. Keek et al. 2006) suggest ignition column depths $\Sigma_{\rm ign} \approx 10^{12}$ g cm^{-2}, where $\Sigma \equiv \int \rho \, {\rm d}z$ is the radially integrated density. Previous superburst ignition models (Cumming & Bildsten 2001; Strohmayer & Brown 2002; Cumming 2003; Brown 2004; Cooper & Narayan 2005; Cumming et al. 2006; Gupta et al. 2007) demonstrated that ^{12}C ignites at $\Sigma \approx 10^{12}$ g cm^{-2} only if ^{12}C is abundant and the ocean temperature $T \approx 6 \times 10^8$ K at that column depth; within existing models of nuclear heating in the neutron star crust, such a large temperature requires an inefficient neutrino emission mechanism in the neutron star core and a low thermal conductivity in the neutron star crust, so that the crust is much hotter than the core.

Recent observations, simulations, and experiments have exposed three fundamental problems with this scenario. First and foremost is the inference that the ocean is in fact too cold for ^{12}C ignition at the inferred column depth $\Sigma_{\rm ign} \approx 10^{12}$ g cm^{-2}. This comes from fits (Shternin et al. 2007; Brown & Cumming 2009) to the quiescent cooling of the quasi-persistent transient KS 1731–260 (Wijnands et al. 2002; Rutledge et al. 2002; Cackett et al. 2006), a system that also exhibited a superburst (Kuulkers et al. 2002b). The timescale for the quiescent luminosity to decrease suggests that the crust's thermal conductivity is high; as a result, the inner crust temperature remains close to that of the core even during the accretion outburst. Cackett et al. (2008) reach the same conclusion for MXB 1659–29 (see also Brown & Cumming 2009). In fact, molecular dynamics simulation results (Horowitz et al. 2007, 2009; Horowitz & Berry 2009) suggest that the neutron star crust is arranged in a regular lattice and therefore has a high thermal conductivity. Neither shear-induced viscous heating (Piro & Bildsten 2007; Keek et al. 2009) nor deep crustal heating due to electron captures, neutron emissions, and pycnonuclear reactions (e.g., Haensel & Zdunik 2008; Horowitz et al. 2008; Gupta et al. 2008) can account for the heat necessary to raise

Electronic address: rcooper@kitp.ucsb.edu; steinera@pa.msu.edu; ebrown@pa.msu.edu

the ocean temperature to the required level (although see Page & Cumming 2005; Blaschke et al. 2008, who consider heating in strange stars and hybrid stars, respectively).

Second, evidence of heavy-ion fusion hindrance at extreme sub-Coulomb-barrier energies (Jiang et al. 2002, 2007, 2008) implies that the cross-section and thereby the $^{12}C+{}^{12}C$ reaction rate may be orders of magnitude smaller than that assumed in the aforementioned superburst ignition models. When included in superburst ignition models, heavy-ion fusion hindrance increases $\Sigma_{\rm ign}$ by at least a factor of 2 (Gasques et al. 2007).

Third, the means by which nuclear burning on the stellar surface produces sufficient quantities of ^{12}C to trigger superbursts is poorly understood. Superburst models require large ^{12}C mass fractions for ignition (Cumming & Bildsten 2001; Cumming 2003; Cooper & Narayan 2005; Cooper et al. 2006; Cumming et al. 2006). All systems that exhibit superbursts show helium-triggered type I X-ray bursts as well (e.g. Galloway et al. 2008), but theoretical models of such bursts yield ^{12}C mass fractions far smaller than those required for ignition (Joss 1978; Schatz et al. 2001, 2003b; Koike et al. 2004; Woosley et al. 2004a; Fisker et al. 2005, 2008; Peng et al. 2007; Parikh et al. 2008). Most systems that exhibit superbursts apparently undergo long periods of stable nuclear burning between successive helium-triggered bursts (Kuulkers et al. 2002a; in 't Zand et al. 2003; Keek et al. 2008); stable burning generates much more ^{12}C than unstable burning, but the calculated yield is insufficient to trigger superbursts in all systems, particularly those accreting at a high rate (Taam & Picklum 1978; Schatz et al. 1999, 2003b; Cooper et al. 2006; Fisker et al. 2006).

Detection of a superburst from the classical transient 4U 1608–522 (Remillard et al. 2005; Kuulkers 2005) with $\Sigma_{\rm ign}\approx 10^{12}$ g cm^{-2} (Keek et al. 2008) exacerbates all three problems: (1) the transient's inferred ocean temperature is lower than those of other systems exhibiting superbursts, (2) heavy ion fusion hindrance is greater at lower temperatures, and (3) most of the matter accreted onto the neutron star prior to the observed superburst likely burned during helium-triggered type I X-ray bursts, which current theoretical calculations suggest would generate far less ^{12}C than that required for ignition.

Reconciling superburst observations with the current theoretical model is impossible. This motivates both a critical assessment of the current ignition model and a search for alternative ignition mechanisms.

Kuulkers et al. (2002b) proposed such an alternative mechanism. Electron captures onto protons and the subsequent captures of the resulting neutrons onto heavy nuclei liberate ≈ 7 MeV$/m_{\rm u}$ (Bildsten & Cumming 1998). Prethreshold captures of super-Fermi electrons are very temperature sensitive and therefore could trigger an energetic thermonuclear flash. An attractive feature of this mechanism is that ignition occurs always at the same electron chemical potential; thus $\Sigma_{\rm ign}$ would be similar for all superbursts, in accord with observations. Unfortunately, the calculated $\Sigma_{\rm ign}\approx 2\times10^{10}$ g cm^{-2} is much smaller than the inferred superburst $\Sigma_{\rm ign}$, making it an unlikely trigger mechanism. This motivates our investigation of exothermic electron captures onto heavy nuclei, which occur throughout the ocean and crust of an accreting neutron star, including the superburst ignition region (Sato 1979; Blaes et al. 1990; Haensel & Zdunik 1990, 2003, 2008; Gupta et al. 2007). In §2 we determine the thermal stability of electron captures onto heavy nuclei in accreting neutron stars. We show that instability requires unrealistically large reaction $\mathcal{Q}$-values, where $\mathcal{Q}$ is the energy released per capture; thus we conclude that electron captures in accreting neutron star oceans are thermally stable. We then consider the relevance of α captures onto light elements such as ^{12}C in §3. We find that none of these reactions is a feasible mechanism and thereby confirm the proposal that $^{12}C+{}^{12}C$ triggers superbursts.

In §4 we assess whether the $^{12}C+{}^{12}C$ reaction rate could be much larger than the fiducial rate. We investigate (§ 4.1) the screening enhancement factor, including a careful evaluation of corrections to the liner mixing rule, and show that uncertainties in the plasma screening enhancement are unlikely to change the $^{12}C+{}^{12}C$ reaction rate enough. We then consider the nuclear cross-section. We find that a strong resonance at an energy near 1.5 MeV in the $^{12}C+{}^{12}C$ system, which theoretical nuclear physics models predict, could increase the reaction rate in the astrophysically relevant temperature range by over two orders of magnitude. In § 5 we show that the existence of such a resonance could decrease the predicted $\Sigma_{\rm ign}$ by a factor $\approx$ 2–4 and thereby alleviate the discrepancy between superburst models and observations. We conclude in §6 by discussing the implications of our findings.

2. THERMAL STABILITY OF ELECTRON CAPTURES

Consider the accretion-driven compression of a matter element containing a nucleus of mass $M(A,Z)$, where A is the mass number and Z is the proton number. The degenerate electrons' chemical potential $\mu_{\rm e}$ rises as the nucleus advects to higher pressures. Eventually $M(A,Z)+\mu_{\rm e}/c^2$ exceeds $M(A,Z-1)$ and electron capture becomes energetically favorable. Such captures often occur in equilibrium and release a negligible amount of energy; however, some captures can heat the ocean in two mutually inclusive ways (e.g. Gupta et al. 2007): (1) An electron captures into an exited state of the daughter nucleus if, for example, the daughter nucleus's ground state is forbidden. The daughter nucleus then radiatively deexcites and thereby heats the ocean. (2) If the parent nucleus is even-even, then $M(A,Z-1)>M(A,Z-2)$ due to the nuclear pairing energy, and a second electron capture immediately ensues. The latter, post-threshold electron capture occurs out of equilibrium and thus releases heat.

2.1. *Governing Equations*

We construct a simple model of the accreted layer to determine the stability of exothermic electron captures to thermal perturbations. We assume spherical accretion onto a neutron star of mass $M=1.4\,M_\odot$ and radius $R=10$ km at an accretion rate per unit area $\dot\Sigma$. The accreted layer's scale height is much less than R, so we set the gravitational acceleration $g=GM/R^2(1-2GM/Rc^2)^{-1/2}=2.43\times10^{14}$ cm s^{-2} throughout the layer. The layer is always in hydrostatic equilibrium, so the column depth Σ is a good Eulerian coordinate. To facilitate comparisons between microphysical and observationally inferred quantities, we express microphysical quantities in terms of the macroscopic coordinate Σ using the following approximate relation between mass density ρ and Σ for relativistic, degenerate electrons[1],

$$\rho\approx 5.9\times10^8\ {\rm g\,cm^{-3}}\left(\frac{\langle A/Z\rangle}{2}\right)\Sigma_{12}^{3/4}, \qquad (1)$$

[1] In this and following expressions, we suppress the scaling with g and evaluate the expressions at $g=2.43\times10^{14}$ cm s^{-2}.

where $\langle A/Z\rangle$ is the mean molecular weight per electron and $\Sigma = \Sigma_{12}\times 10^{12}$ g cm^{-2}. We denote the Eulerian time and spatial derivatives as $\partial/\partial t$ and $\partial/\partial\Sigma$, respectively, and the Lagrangian derivative following a matter element as D/Dt, where $D/Dt = \partial/\partial t + \dot{\Sigma}\partial/\partial\Sigma$. The governing transport, entropy, and continuity equations are

$$F = \rho K\frac{\partial T}{\partial\Sigma}, \tag{2}$$

$$T\frac{Ds}{Dt} = \mathcal{E}Xr_{\rm ec} + \frac{\partial F}{\partial\Sigma}, \tag{3}$$

$$\frac{DX}{Dt} = -Xr_{\rm ec}, \tag{4}$$

where F is the flux, K is the thermal conductivity, s is the entropy, $\mathcal{E} = \mathcal{Q}/(Am_{\rm u})$ is the energy per gram released via electron captures, X is the parent nucleus mass fraction,

$$r_{\rm ec} = \left(\frac{\ln 2}{\langle ft\rangle}\right)\frac{1}{(m_{\rm e}c^2)^5}\int_Q^\infty E^2(E-Q)^2 f(E,\mu_{\rm e},T)dE \tag{5}$$

is the electron capture rate (Fuller et al. 1985), $\langle ft\rangle$ is the effective ft value (Fuller et al. 1980, 1985; Langanke & Martínez-Pinedo 2001), $m_{\rm e}$ is the electron mass, Q is the threshold energy, and

$$f(E,\mu_{\rm e},T) = \frac{1}{1+\exp[(E-\mu_{\rm e})/k_{\rm B}T]} \tag{6}$$

is the Fermi-Dirac distribution function.

Consider prethreshold electron captures, where $\mu_{\rm e} < Q$. For $T = 0$, all electrons have energies $E \le \mu_{\rm e}$ by equation (6); electron capture is blocked. For $T > 0$ some electrons have $E > Q$ and thus can capture. The number of electrons with $E > Q$ increases with T, which makes prethreshold electron capture temperature-sensitive. In the prethreshold limit $(\mu_{\rm e} - Q)/k_{\rm B}T \ll 0$,

$$r_{\rm ec}(\mu_{\rm e},T) = \left(\frac{\ln 2}{\langle ft\rangle}\right)\frac{2Q^2(k_{\rm B}T)^3}{(m_{\rm e}c^2)^5}\exp\left[-\left(\frac{Q-\mu_{\rm e}}{k_{\rm B}T}\right)\right] \tag{7}$$

(Fuller et al. 1985; Bildsten & Cumming 1998). Conversely, for $\mu_{\rm e} > Q$ a majority of electrons has $E > Q$ and hence can capture for any T, making $r_{\rm ec}$ relatively temperature-insensitive and thus thermally stable. We therefore consider prethreshold electron captures exclusively hereafter.

2.2. *Prethreshold Electron Capture*

Prethreshold electron captures occur within a thin layer in the deep ocean. To illustrate this, consider the height-integrated capture rate. Relativistic, degenerate electrons supply the pressure $P = g\Sigma$, so

$$\Sigma \approx \frac{\mu_{\rm e}^4}{12\pi^2 g(\hbar c)^3} = 10^{12}\ {\rm g\,cm^{-2}}\left(\frac{\mu_{\rm e}}{3.43\ {\rm MeV}}\right)^4. \tag{8}$$

Integrating equation (7) over Σ and using equation (8),

$$\int_0^{\mu_{\rm e}} r_{\rm ec}(\mu_{\rm e}',T)\,d\Sigma' \approx \left(\frac{4k_{\rm B}T}{\mu_{\rm e}}\right)r_{\rm ec}(\mu_{\rm e},T)\Sigma \tag{9}$$

for $\mu_{\rm e} \gg k_{\rm B}T$. Equation (9) shows that prethreshold electron captures occur in a narrow column depth range

$$\frac{\Delta\Sigma}{\Sigma} \approx \frac{4k_{\rm B}T}{\mu_{\rm e}} = 0.050\left(\frac{T_8}{5}\right)\Sigma_{12}^{-1/4}, \tag{10}$$

where $T = T_8\times 10^8$ K.

Now consider electron captures in steady-state, such that electrons capture onto nuclei at the same rate as accretion advects the nuclei (see also the discussion in Bildsten & Cumming 1998). Equation (4) becomes

$$\dot{\Sigma}\frac{\partial\ln X}{\partial\Sigma} = -r_{\rm ec}. \tag{11}$$

Integrating equation (11) from 0 to Q and using equations (8) and (9), we find that most electron captures occur prethreshold when

$$\Sigma_{12} > 0.027\left(\frac{T_8}{5}\right)^{-16/5}\left(\frac{\dot{\Sigma}}{0.3\dot{\Sigma}_{\rm Edd}}\right)^{4/5}\left(\frac{\langle ft\rangle}{10^3\ {\rm s}}\right)^{4/5}, \tag{12}$$

where $\dot{\Sigma}_{\rm Edd}\approx 10^5$ g cm^{-2} s^{-1} is the local accretion rate at which the accretion flux equals the Eddington flux[2]. Superbursts ignite at column depths $\Sigma_{12}\sim 1$ and accretion rates $\dot{\Sigma}\approx 0.1$–$1\ \dot{\Sigma}_{\rm Edd}$. Equation (12) shows that superallowed electron captures (for which $\langle ft\rangle\sim 10^3$–$10^4$ s) occur prethreshold at superburst ignition depths.

2.3. *Thermal Stability Analysis*

We now derive a one-zone model (e.g., Fujimoto et al. 1981; Paczyński 1983; Bildsten 1998b) from the governing equations (2-4) to determine the stability of prethreshold electron captures to thermal perturbations and thereby ascertain whether electron captures trigger superbursts. We consider only temperature perturbations and ignore the accretion-induced entropy advection through the bottom of the zone. Therefore, we set $\partial/\partial t = 0$ in equation (4) and approximate $Ds/Dt = \partial s/\partial t$ in equation (3). Perturbations occur at constant pressure since the scale height $\sim\Sigma/\rho \ll R$; therefore, we write $Tds = C_P dT$, where C_P is the specific heat at constant pressure. Equations (2-4) become

$$F = \rho K\frac{\partial T}{\partial\Sigma}, \tag{13}$$

$$C_P\frac{\partial T}{\partial t} = \mathcal{E}Xr_{\rm ec} + \frac{\partial F}{\partial\Sigma}, \tag{14}$$

$$\dot{\Sigma}\frac{\partial X}{\partial\Sigma} = -Xr_{\rm ec}. \tag{15}$$

We simplify equations (13-15) as follows. We set ρ, F, and X to be constant throughout the layer; specifically, we adopt step-like profiles for F and X:

$$F(\Sigma,t) = F_0(t)\Theta(\Sigma_{\rm ec}-\Sigma),\quad X(\Sigma) = X_0\Theta(\Sigma_{\rm ec}-\Sigma), \tag{16}$$

where Θ is the Heaviside step function, $\Sigma_{\rm ec}$ denotes the column depth at the bottom of the layer, and F_0 and X_0 denote the values at the top of the layer, where $\Sigma \ll \Sigma_{\rm ec}$. We assume the ocean consists of a single ion species and set $X_0 = 1$. Electron-ion scattering sets the ocean's thermal conductivity (Yakovlev & Urpin 1980; Itoh et al. 1983; Potekhin et al. 1999)

$$K \approx \frac{9.8\times 10^{18}}{Z^{2/3}A^{1/3}}\left(\frac{T_8}{5}\right)\left(\frac{\rho}{6\times 10^8\ {\rm g\,cm^{-3}}}\right)^{1/3}\ {\rm ergs\ cm^{-1}\ s^{-1}\ K^{-1}}, \tag{17}$$

[2] We define the Eddington luminosity to be $4\pi GMc/\kappa_{\rm es}$ in the frame of a distant observer. This is the largest luminosity observable by such an observer (see Shapiro & Teukolsky 1983). This differs from the definition used by Galloway et al. (2008) by a factor of $[1-2GM/(Rc^2)]^{-1/2} = 1.3$.

where we set the Coulomb logarithm $\Lambda_{ei} = 1$, a value appropriate for a plasma at $T_8 \approx 5$ and $\rho \approx 6 \times 10^8$ g cm^{-3}. Since $K \propto T$, we rewrite equation (13) as

$$F = \frac{\rho K}{2T}\frac{\partial T^2}{\partial \Sigma}. \quad (18)$$

Equations (16) and (18) then imply

$$T^2(\Sigma,t) = T_0^2 + \left[T_{ec}(t)^2 - T_0^2\right]\frac{\Sigma}{\Sigma_{ec}}. \quad (19)$$

Integrating equations (14-15) over Σ and using equations (9), (10), (16), (18), and (19), we find

$$C_P\frac{\partial T_{ec}}{\partial t} = \frac{\Delta\Sigma}{\Sigma_{ec}}\mathcal{E}r_{ec} - \frac{\rho K}{2T}\left(\frac{T_{ec}^2 - T_0^2}{\Sigma_{ec}^2}\right), \quad (20)$$

$$r_{ec} = \frac{\dot{\Sigma}}{\Delta\Sigma}. \quad (21)$$

Equation (21) shows that electron capture occurs when the lifetime of a parent nucleus $1/r_{ec}$ equals the time $t_{acc}\Delta\Sigma/\Sigma$ an advecting element spends within the capture region, where

$$t_{acc} \equiv \Sigma/\dot{\Sigma} \quad (22)$$

is the accretion timescale. Note that this differs from the usual assumption (Blaes et al. 1990; Bildsten 1998a; Bildsten & Cumming 1998; Ushomirsky et al. 2000) that electron capture occurs when $1/r_{ec} = t_{acc}$.

Finally, conducting a linear stability analysis on equation (20) and using equation (21), the thermal instability criterion is

$$\nu\frac{\mathcal{E}}{t_{acc}} > \frac{\rho K T_{ec}}{\Sigma_{ec}^2}, \quad (23)$$

where the temperature-sensitivity of the height-integrated electron capture rate

$$\nu \equiv \frac{\partial \ln(r_{ec}\Delta\Sigma)}{\partial \ln T} = 4 + \ln\left[8\ln 2\frac{t_{acc}}{\langle ft\rangle}\frac{Q^2(k_BT)^4}{(m_ec^2)^5\mu_e}\right] \quad (24)$$

from equations (7) and (9). Noting that electrons capture when $\mu_e/Q \approx 1$, we write equation (24) as

$$\nu = 8.14 + \ln\left[\left(\frac{T_8}{5}\right)^4\Sigma_{12}^{5/4}\left(\frac{\dot{\Sigma}}{0.3\dot{\Sigma}_{Edd}}\right)^{-1}\left(\frac{\langle ft\rangle}{10^3\ \mathrm{s}}\right)^{-1}\right]. \quad (25)$$

Using equations (22) and (17), the thermal instability criterion (23) becomes

$$\left(\frac{\nu}{8.14}\right)\mathcal{Q} > 20\left(\frac{T_8}{5}\right)^2\left(\frac{\dot{\Sigma}}{0.3\dot{\Sigma}_{Edd}}\right)^{-1}\left(\frac{A}{2Z}\right)^2 \mathrm{MeV}, \quad (26)$$

where $\mathcal{Q}$ is the energy released per electron capture.

We tested the accuracy of equation (23) using the suitably modified global linear stability analysis of Cooper & Narayan (2005). The minimum $\mathcal{Q}$ for instability derived from the global stability analysis differed from that of equation (26) by less than 30% for each of the 12 test cases.

Typically $\mathcal{Q} < Q$ because the daughter nucleus is generally more massive than the parent nucleus, although exceptions exist. Gupta et al. (2007) find $\mathcal{Q} < 6.2$ MeV for all electron captures that occur for $\mu_e < 6$ MeV, or equivalently, $\Sigma_{12} < 10$ (eq. [8]). From equation (26), it follows that electron captures are thermally stable for the accretion rates and column depths at which superbursts occur. Therefore, we conclude that electron captures do not trigger superbursts.

3. ALTERNATIVE FUSION REACTIONS

In this section, we examine whether light-element fusion reactions trigger superbursts. Hydrogen has an electron capture threshold energy $Q = 1.2933$ MeV and thus depletes at $\Sigma_{12} \lesssim 2 \times 10^{-2}$ (eq. [8]). The helium abundance at Σ_{ign} is less certain, and we discuss it below. The paucity of stable isotopes of $Z = 3$–5 nuclei leaves ^{12}C as the next reasonable alternative, which we address in §4. Finally, nuclei with $Z > 6$ are unlikely candidates because the extra Coulomb repulsion causes the fusion rates to be significantly lower than that of ^{12}C.

Thus, other than ^{12}C + ^{12}C, α capture reactions such as ^{12}C$(\alpha,\gamma)^{16}$O are the only plausible fusion reactions that might trigger superbursts. The conditions for these reactions to produce superbursts are similar to those for electron captures, namely, that (1) the reaction rate r_{nuc} is sufficiently temperature dependent to produce unstable burning, and (2) α particles must survive to the inferred Σ_{ign}. Below, we show that the latter condition is not met; thus α particles deplete too quickly to trigger superbursts.

The condition for α particles to survive at a column depth Σ is $Y/\sum_i (r_{nuc})_i > \Sigma/\dot{\Sigma}$ (see §2.3), where Y is the helium mass fraction and the sum is over all reactions that consume α particles. Using the triple-α reaction rate of Fushiki & Lamb (1987) and setting $\rho = 6 \times 10^8$ g cm^{-3}, $T_8 = 5$, and $Y = 1$, we find $r_{nuc} = 2.2 \times 10^6$ s^{-1}, which implies a lifetime of 4.6×10^{-7} s. The reaction rate $r_{nuc} \propto Y^3$, so the lifetime is much larger for smaller helium abundances. The accretion timescale $t_{acc} = 10^7[\Sigma_{12}/(\dot{\Sigma}/\dot{\Sigma}_{Edd})]$ s (eq. [22]), indicating that $Y < 10^{-7}$ for helium to survive. At this low Y, the rise in temperature from consuming the helium via, e.g., ^{12}C(α,γ), is $\lesssim 10^6$ K $\ll T$ and hence insufficient to trigger a thermal instability.

From the results of this section and §2, we conclude that ^{12}C fusion triggers superbursts.

4. THE ^{12}C + ^{12}C REACTION RATE

A possible solution to the superburst ignition problem is that the true ^{12}C + ^{12}C fusion rate is larger than assumed. ^{12}C ignition at the inferred Σ_{ign} requires a $\sim 10^4$ reaction rate enhancement for an ocean temperature of 4×10^8 K (Cumming et al. 2006) or a $\sim 10^2$ enhancement for 5×10^8 K. The two sources of uncertainty in the fusion rate are (1) plasma screening effects and (2) the nuclear cross-section $\sigma(E)$. In the following subsections, we investigate whether either source could account for such a large increase in the fusion rate.

4.1. *Plasma Screening*

Superbursts ignite in a strongly-coupled Coulomb plasma. Two dimensionless parameters determine the plasma's state. The first is the Coulomb coupling parameter

$$\Gamma \equiv \frac{Z^2e^2}{ak_BT} = 6.0\left(\frac{T_8}{5}\right)^{-1}\Sigma_{12}^{1/4}\left(\frac{Z}{6}\right)^{5/3}, \quad (27)$$

where $a = (3Z/4\pi n_e)^{1/3}$ is the ion-sphere radius, n_e is the electron number density, and we used equation (1), which assumes the gravitational acceleration $g = 2.43 \times 10^{14}$ cm s^{-2}. For $\Gamma \ll 1$ Coulomb coupling is weak and the ions constitute a Maxwell-Boltzmann gas. As Γ increases, the ions gradually become a Coulomb liquid. When $\Gamma > 175$ the ions crystallize (Potekhin & Chabrier 2000). Equation (27) implies that

superbursts ignite in a Coulomb liquid. The second dimensionless parameter,

$$\zeta \equiv \frac{3\Gamma}{\tau} \approx 0.17 \left(\frac{T_8}{5}\right)^{-2/3} \Sigma_{12}^{1/4} \left(\frac{2Z}{A}\right)^{1/3}, \quad (28)$$

is the ratio of the classical turning point to the ion separation, where

$$\tau = \left(\frac{27\pi^2 \mu Z^4 e^4}{2k_{\rm B}T\hbar^2}\right)^{1/3} = \left(\frac{27\pi^2 A m_{\rm u} Z^4 e^4}{4k_{\rm B}T\hbar^2}\right)^{1/3} \quad (29)$$

and μ is the reduced mass of the reacting nuclei. Specifically, $\zeta = r_{\rm TP}/a$, where $r_{\rm TP}$ is the radius at which the Coulomb energy $Z^2e^2/r_{\rm TP}$ equals the classical Gamow peak energy (Clayton 1983)

$$E^{\rm pk} = \frac{\tau k_{\rm B}T}{3}. \quad (30)$$

Many-body interactions in a strongly-coupled Coulomb plasma modify the Coulomb potential between two reacting nuclei (for a review, see Ichimaru 1993). From these many-body interactions, one derives an effective two-body potential

$$V(r) = \frac{Z^2e^2}{r} - H(r), \quad (31)$$

where r is the distance between the reacting nuclei. From $H(r)$, one derives the plasma screening enhancement to the reaction rate $\exp(\langle H(r)\rangle/k_{\rm B}T)$, where $\langle H(r)\rangle$ is a path-integral average of $H(r)$ (e.g. Ichimaru 1993). One can expand the static mean-field potential $H(r)$ as a power series in $(r/a)^2$ (Widom 1963). Neglecting quantum effects in $H(r)$, the leading order term $H(0)$ is a thermodynamic quantity; $H(0)$ equals the difference between the Coulomb (or excess) Helmholtz free energy before and after the reaction (DeWitt et al. 1973).

Monte Carlo simulations and hypernetted chain calculations of binary ionic mixtures (Hansen & Vieillefosse 1976; Hansen et al. 1977; Chabrier & Ashcroft 1990; Ogata et al. 1993; Rosenfeld 1995, 1996; DeWitt et al. 1996; DeWitt & Slattery 2003) suggest the excess free energy obeys the linear mixing rule to high accuracy in the regime $\Gamma > 1$ (Potekhin et al. 2009). Therefore, authors usually invoke the linear mixing rule when deriving the plasma screening enhancement to the reaction rate. In this case, the total free energy of an ionic mixture

$$\frac{F^{\rm ex}}{k_{\rm B}T} = \sum_i N_i f^{\rm ex}(\Gamma_i), \quad (32)$$

where N_i is the number of ions with charge Z_i, $f^{\rm ex} \equiv F^{\rm ex,OCP}/Nk_{\rm B}T$ is the well-determined reduced excess free energy per ion of a one-component plasma (e.g., Chabrier & Potekhin 1998; Potekhin & Chabrier 2000), and $\Gamma_i \propto Z_i^{5/3}$ is the Coulomb coupling parameter for species i (eq. [27]).

From equation (32), $H(0)/k_{\rm B}T = 2f^{\rm ex}(\Gamma) - f^{\rm ex}(2^{5/3}\Gamma)$ (Jancovici 1977, see also the Appendix), where Γ is that of the reacting ions; using the ion-sphere model result $f^{\rm ex} \approx -0.9\Gamma$ (Salpeter 1954), $H(0)/k_{\rm B}T = 0.9(2^{5/3}-2)\Gamma \approx 1.0573\Gamma$, so the lowest-order screening enhancement to the ^{12}C + ^{12}C reaction rate

$$\exp\left(\frac{H(0)}{k_{\rm B}T}\right) = 5.5\times10^2 \exp\left[\left(\frac{T_8}{5}\right)^{-1}\Sigma_{12}^{1/4} - 1\right]. \quad (33)$$

Despite its simplicity, equation (33) is adequate for most applications (Gasques et al. 2005; Yakovlev et al. 2006; Chugunov et al. 2007). We discuss corrections to the screening enhancement below.

4.1.1. *Deviation from Linear Mixing Rule*

The excess free energy $F^{\rm ex}$ of a multicomponent plasma exhibits small deviations from the linear mixing rule (eq. [32]). In general,

$$\frac{F^{\rm ex}}{k_{\rm B}T} = \sum_i N_i f^{\rm ex}(\Gamma_i) + N\Delta f^{\rm ex}, \quad (34)$$

where $\Delta f^{\rm ex} \geq 0$ is a function of both the charges Z_i and concentrations $x_i \equiv N_i/N$ of the ionic species (e.g., DeWitt et al. 1996). Using the hypernetted chain calculations of DeWitt et al. (1996) and the ansatz $\Delta f^{\rm ex} \propto x_1x_2(Z_2/Z_1)^{3/2}$ (DeWitt & Slattery 2003), we find

$$\Delta f^{\rm ex} = (0.0091\ln\Gamma_1 + 0.018)x_1x_2\left(\frac{Z_2}{Z_1}\right)^{3/2} \quad (35)$$

for a binary ionic mixture (see also Potekhin et al. 2009).

To incorporate linear mixing rule deviations into $H(0)$ calculations, previous authors assumed a one-component plasma (consisting of ^{12}C ions in this case). Fusion of two ^{12}C ions generates a compound nucleus ^{24}Mg and thereby forms a binary ionic mixture. One determines $H(0)$ by finding the difference in $F^{\rm ex}$ before and after the reaction in the limit that the compound nucleus concentration $x_2 \to 0$ (Ichimaru 1993). Using this assumption and equations (34) and (35), we find the correction to $H(0)$:

$$\frac{\Delta H(0)}{k_{\rm B}T} = -0.026\ln\Gamma - 0.051, \quad (36)$$

in good agreement with DeWitt et al. (1996); for a one-component plasma, linear mixing rule deviations reduce the plasma screening enhancement factor by $\sim 10\%$.

However, the plasma at the superburst ignition depth is likely a mixture of ^{12}C and heavier ions with $Z \lesssim 46$ (e.g., Koike et al. 1999, 2004; Schatz et al. 2001, 2003b; Woosley et al. 2004a). Generalizing equation (35) for a multicomponent plasma with $Z_i < Z_j$ for $i < j$, we find (Ogata et al. 1993)

$$\Delta f^{\rm ex} = \sum_{i<j} x_ix_j\Delta f_{ij}^{\rm ex}; \quad \Delta f_{ij}^{\rm ex} = (0.0091\ln\Gamma_i + 0.018)\left(\frac{Z_j}{Z_i}\right)^{3/2}. \quad (37)$$

To illustrate the effect spectator ions have on the screening enhancement, consider for simplicity a ternary ionic mixture of ^{12}C, ^{24}Mg, and a representative spectator ion ^{56}Fe. Using equations (34) and (37) and again taking the ^{24}Mg concentration $x_2 \to 0$, so that $x_1 + x_3 = 1$, we find (see Appendix)

$$\frac{\Delta H(0)}{k_{\rm B}T} = -\Delta f_{12}^{\rm ex} + x_3\left[\Delta f_{12}^{\rm ex} + (1+x_3)\Delta f_{13}^{\rm ex} - \Delta f_{23}^{\rm ex}\right]. \quad (38)$$

Note that equation (38) reduces to (36) in the limit $x_3 \to 0$, as it should. Equation (38) shows that, since the bracketed term is positive, heavy spectator ions *increase* the screening enhancement factor (i.e. $\partial\Delta H(0)/\partial x_3 > 0$). For the fiducial ^{12}C mass fraction 0.2 and ^{56}Fe mass fraction 0.8 (such that $x_1 = 7/13$ and $x_3 = 6/13$; Cumming et al. 2006), linear mixing rule deviations increase the plasma screening enhancement by $\approx 10\%$.

Potekhin et al. (2009) developed an analytic formula for $\Delta f^{\rm ex}$ that is more accurate than equation (37). We derive the corresponding formula for $\Delta H(0)/k_{\rm B}T$ in the Appendix. In Figure 1, we plot $\Delta H(0)/k_{\rm B}T$ as a function of the spectator ion number fraction x_3 using both equation (38) and the

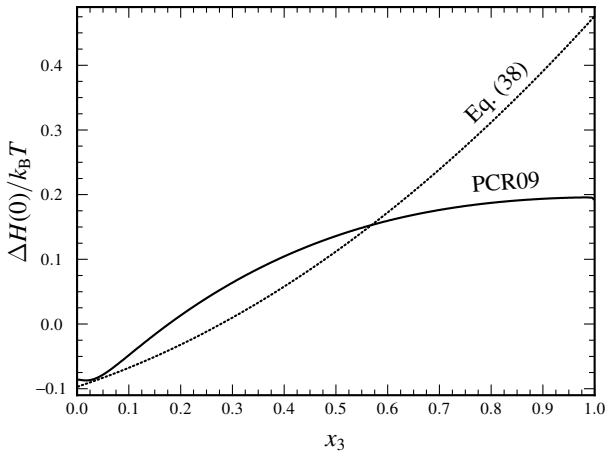

FIG. 1.— Correction to the plasma screening enhancement factor due to linear mixing rule deviations as a function of the spectator ion number fraction x_3. Considered is a ternary ionic mixture with $Z_1 = 6$, $Z_2 = 12$, $Z_3 = 26$, and $\Gamma_1 = 6$. The number fraction of the product ion $x_2 = 0$, so $x_1 = 1 - x_3$. "PCR09" refers to the expression for $\Delta H(0)/k_BT$ derived from the results of Potekhin et al. (2009, see Appendix).

expression derived from Potekhin et al. (2009). Figure 1 confirms that heavy spectator ions increase the plasma screening enhancement to the reaction rate, although the two expressions for $\Delta H(0)/k_BT$ differ quantitatively.

4.1.2. *Corrections to* $\langle H(r)\rangle$

The next term in the expansion of $H(r)$ goes as $(r/a)^2 \propto \zeta^2$; its contribution is small because $\zeta^2 \ll 1$ (eq. [28]). From Jancovici (1977), we find

$$\frac{\langle H(r)\rangle - H(0)}{k_BT} \approx -\frac{5}{32}\Gamma\zeta^2 = -0.027\left(\frac{T_8}{5}\right)^{-7/3}\Sigma_{12}^{3/4}. \quad (39)$$

This result agrees very well with more accurate calculations (Alastuey & Jancovici 1978; Ogata et al. 1991; Ogata 1997). Higher order terms are even smaller; therefore, we conclude that corrections to $\langle H(r)\rangle$ are unimportant in calculating the plasma screening enhancement for ^{12}C ignition.

4.1.3. *Electron Screening Corrections*

In the above analysis, we tacitly assumed a uniform electron density. Although highly degenerate, electrons nonetheless slightly concentrate around positively charged ions. Electron polarization mitigates the Coulomb repulsion between ions relative to an unpolarized configuration. This has two counteracting effects: It (1) lowers the Coulomb repulsion between the two reacting ions, which increases the reaction rate, and (2) attenuates the many-body Coulomb interactions and thereby $H(r)$, which decreases the reaction rate. The Yukawa potential $Z^2e^2/r\exp(-r/r_{TF})$ describes the two-body potential, where r_{TF} is the Thomas-Fermi screening length. For relativistic, degenerate electrons, $r_{TF}/a = 3.0(Z/6)^{-1/3}$ (e.g., Haensel et al. 2007), so electron screening is weak; from the results of Sahrling & Chabrier (1998), electron screening changes the reaction rate by $\lesssim 1\%$.

Corrections to the lowest-order plasma screening enhancement (eq. [33]) change the ^{12}C + ^{12}C reaction rate by a factor < 2. Therefore, we conclude that uncertainties in the plasma screening enhancement are too small to explain the discrepancy between superburst observations and theoretical model results.

4.2. *The Nuclear Cross-Section*

Although the plasma screening enhancement to the ^{12}C + ^{12}C reaction rate is well-determined for superburst conditions, the nuclear cross-section $\sigma(E)$ is not. Many groups have measured $\sigma(E)$ at various center-of-mass energies E down to ≈ 2.1 MeV (Patterson et al. 1969; Mazarakis & Stephens 1972, 1973; Spinka & Winkler 1974; High & Čujec 1977; Kettner et al. 1977, 1980; Erb et al. 1980; Treu et al. 1980; Becker et al. 1981; Dasmahapatra et al. 1982; Satkowiak et al. 1982; Rosales et al. 2003; Barrón-Palos et al. 2004, 2006; Aguilera et al. 2006; Spillane et al. 2007). However, the energy range of interest is centered at the classical Gamow peak energy (cf. eq. [29–30])

$$E^{pk} = 1.5\left(\frac{T_8}{5}\right)^{2/3}\ \text{MeV} \quad (40)$$

and has a full width

$$\Delta E^{pk} = 4\left(\frac{E^{pk}k_BT}{3}\right)^{1/2} = 0.59\left(\frac{T_8}{5}\right)^{5/6}\ \text{MeV}. \quad (41)$$

Thus, $\sigma(E)$ in the astrophysically relevant energy range is experimentally unknown.

This situation is common in nuclear astrophysics: to determine the astrophysical reaction rate, one either extrapolates the experimental data to lower energies or calculates the rate theoretically (e.g., Caughlan & Fowler 1988; Gasques et al. 2005). In doing so, one tacitly assumes the astrophysical rate has the nonresonant form, i.e., no prominent resonances exist in the compound nucleus within the relevant energy range[3]. However, several groups have detected strong resonances in the ^{12}C + ^{12}C system at energies below the Coulomb barrier. Resonances exist throughout the entire energy range probed so far, and the spacing between adjacent resonances[4] is ≈ 0.3 MeV. Therefore, a resonance probably exists near E^{pk} (Bromley et al. 1960; Almqvist et al. 1960; Galster et al. 1977; Korotky et al. 1979; Erb et al. 1980; Treu et al. 1980; Spillane et al. 2007). Indeed, Michaud & Vogt (1972) and Perez-Torres et al. (2006) predict a resonance exists in the ^{12}C + ^{12}C system with energy $E_R \approx 1.5$ MeV. If the resonance is strong, the thermally averaged reaction rate $\langle\sigma v\rangle$ would be much larger than assumed.

To illustrate the effect a strong resonance within the Gamow window would have on the ^{12}C + ^{12}C reaction rate, we follow the prediction of Perez-Torres et al. (2006) and assume the existence of a single, narrow resonance with $E_R = 1.5$ MeV. Then

$$\langle\sigma v\rangle = \langle\sigma v\rangle_{NR} + \langle\sigma v\rangle_R, \quad (42)$$

$$\langle\sigma v\rangle_R = \left(\frac{\pi}{3m_uk_BT}\right)^{3/2}\hbar^2(\omega\gamma)_R\exp\left(-\frac{E_R}{k_BT}\right), \quad (43)$$

[3] This statement is not strictly true for heavy ion fusion reactions such as ^{12}C + ^{12}C. The compound nucleus ^{24}Mg has numerous quasi-stationary states at excitation energies near 15 MeV above the ground state (Endt 1990; Firestone 2007), where E^{pk} lies; thus all reactions are resonant. However, when the mean level spacing of quasi-stationary states $D \lesssim k_BT$, one computes an average cross-section over all resonances, and the reaction rate assumes the nonresonant form (e.g. Cameron 1959; Fowler & Hoyle 1964)

[4] The average level spacing of the detected resonances is much greater than that of the quasi-stationary states in the compound nucleus ^{24}Mg. Thus the observed resonances are not ordinary compound nuclear states. As Almqvist et al. (1960) first suggested, the resonances are probably quasi-molecular doorway states in the ^{12}C + ^{12}C system (e.g., Betts & Wuosmaa 1997).

where $\langle\sigma v\rangle_{\rm NR}$ is the nonresonant contribution to the total reaction rate as given in, e.g., Caughlan & Fowler (1988), $\langle\sigma v\rangle_{\rm R}$ is the resonant contribution,

$$(\omega\gamma)_{\rm R} = 2(2J+1)\frac{\Gamma_{\rm C}(\Gamma_{\rm R}-\Gamma_{\rm C})}{\Gamma_{\rm R}} \approx 2(2J+1)\Gamma_{\rm C} \qquad (44)$$

is the resonance strength, J is the total angular momentum of the resonance, $\Gamma_{\rm C}$ is the entrance channel width, and $\Gamma_{\rm R} \gg \Gamma_{\rm C}$ is the resonance width.

The resonant contribution $\langle\sigma v\rangle_{\rm R} \propto (\omega\gamma)_{\rm R}$. Using the Breit-Wigner single resonance formula,

$$\sigma(E) = \frac{\pi\hbar^2}{12Em_{\rm u}}\frac{(\omega\gamma)_{\rm R}\Gamma_{\rm R}}{(E-E_{\rm R})^2+(\Gamma_{\rm R}/2)^2} \qquad (45)$$

(e.g., Clayton 1983). Evaluating equation (45) at $E = E_{\rm R}$,

$$(\omega\gamma)_{\rm R} = 3.4\times10^{-8}\left(\frac{\Gamma_{\rm R}}{100\,{\rm keV}}\right)\left(\frac{\sigma(E_{\rm R})}{10^{-13}\,{\rm barn}}\right)\left(\frac{E_{\rm R}}{1.5\,{\rm MeV}}\right)\,{\rm eV}, \qquad (46)$$

where we normalize the resonance width $\Gamma_{\rm R}$ to that typical of known resonances (see, e.g., Table IV of Aguilera et al. 2006) and the cross-section at resonance $\sigma(E_{\rm R})$ to the approximate value Perez-Torres et al. (2006) predict. For this work, we adopt $(\omega\gamma)_{\rm R} = 3.4\times10^{-8}$ eV as the fiducial resonance strength.

To determine an upper limit for $(\omega\gamma)_{\rm R}$, we demand that the resonance's contribution to the astrophysical S-factor at a given energy E, $S_{\rm R}(E)$, be less than the experimentally measured value $S_{\rm exp}(E)$ for all $E \gtrsim 2.1$ MeV, the lowest energy probed at the time of this writing. The S-factor for ^{12}C + ^{12}C is

$$S(E) = \sigma(E)E\exp\left[87.21\left(\frac{E}{\rm MeV}\right)^{-1/2}+0.46\left(\frac{E}{\rm MeV}\right)\right] \qquad (47)$$

(Patterson et al. 1969; Clayton 1983). From equations (45) and (47), we write

$$S_{\rm R}(E) = S(E_{\rm R})\frac{(\Gamma_{\rm R}/2)^2}{(E-E_{\rm R})^2+(\Gamma_{\rm R}/2)^2}. \qquad (48)$$

Using equations (45), (47), and (48), demanding that $S_{\rm R}(E) < S_{\rm exp}(E)$, and noting that $(E-E_{\rm R})^2 \gg (\Gamma_{\rm R}/2)^2$, we find

$$(\omega\gamma)_{\rm R} < 5.5\times10^{-8}\left(\frac{\Gamma_{\rm R}}{100\,{\rm keV}}\right)^{-1} \times\left[\left(\frac{E-E_{\rm R}}{\rm MeV}\right)^2\left(\frac{S_{\rm exp}(E)}{10^{16}\,{\rm MeV\,barn}}\right)\right]\,{\rm eV} \qquad (49)$$

for a resonance at $E_{\rm R} = 1.5$ MeV. Equation (49) must be satisfied for all E. According to the experimental data, the minimum value of the bracketed term is ≈ 1 (see, e.g., Fig. 4 of Spillane et al. 2007), so

$$(\omega\gamma)_{\rm R} < 5.5\times10^{-8}\left(\frac{\Gamma_{\rm R}}{100\,{\rm keV}}\right)^{-1}\,{\rm eV}. \qquad (50)$$

If $\Gamma_{\rm R} \approx 100$ keV, then our fiducial strength $(\omega\gamma)_{\rm R} = 3.4\times10^{-8}$ eV is comparable to the maximum possible strength. $\Gamma_{\rm R}$ may be much smaller, however; the resonance at 2.14 MeV, the lowest-energy resonance known as of this writing, has a width $\Gamma_{\rm R} < 12$ keV (Spillane et al. 2007). Therefore, we set $(\omega\gamma)_{\rm R} = 3.4\times10^{-7}$ eV, which is ten times larger than our fiducial rate, as a reasonable upper limit.

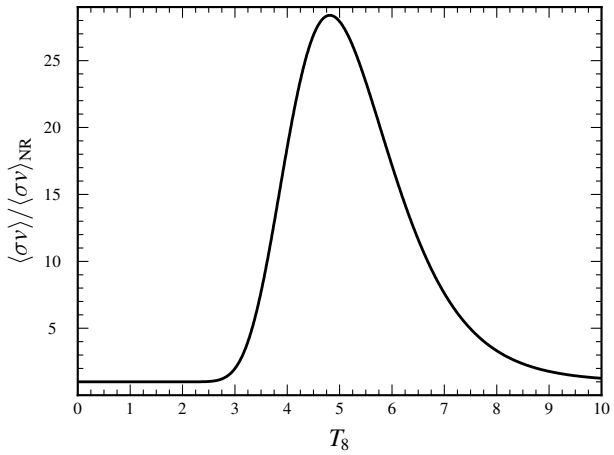

FIG. 2.— Ratio of the total thermally averaged reaction rate $\langle\sigma v\rangle = \langle\sigma v\rangle_{\rm NR} + \langle\sigma v\rangle_{\rm R}$ to the nonresonant contribution $\langle\sigma v\rangle_{\rm NR}$ for a hypothetical 1.5 MeV resonance with strength $(\omega\gamma)_{\rm R} = 3.4\times10^{-8}$ eV, the fiducial value, as a function of temperature $T = T_8\times10^8$ K. The resonance increases $\langle\sigma v\rangle$ by a factor $\gtrsim 25$ near $T_8 \approx 5$.

Figure 2 shows the effect a 1.5 MeV resonance has on the reaction rate $\langle\sigma v\rangle$. For the fiducial $(\omega\gamma)_{\rm R}$ value, the resonance increases $\langle\sigma v\rangle$ by a factor $\gtrsim 25$ at temperatures relevant to superbursts; for the $(\omega\gamma)_{\rm R}$ upper limit, the resonance increases $\langle\sigma v\rangle$ by a factor $\gtrsim 250$. These increases are of the order required to reconcile the observationally inferred $\Sigma_{\rm ign}$ with that calculated from theoretical models for a specific range of assumed crust thermal conductivities and core neutrino emissivities. In the following section, we compute the superburst $\Sigma_{\rm ign}$ with the effect of this resonance.

5. EFFECTS OF A RESONANCE ON SUPERBURST IGNITION

We use the global linear stability analysis of Cooper & Narayan (2005) to determine the effect a strong resonance in the ^{12}C + ^{12}C system would have on the superburst ignition depth $\Sigma_{\rm ign}$. We assume steady spherical accretion onto a neutron star of mass $M = 1.4\,M_\odot$ and radius $R = 10$ km. The accreted matter composition is that of the Sun: The hydrogen mass fraction $X = 0.7$, helium mass fraction $Y = 0.28$, and heavy-element mass fraction $Z = 0.02$. Furthermore, we follow Cumming et al. (2006) and assume the ^{12}C mass fraction $X_{\rm C} = 0.2$ at the base of the accreted layer.

We make the following two modifications to the model of Cooper & Narayan (2005). (1) Cooper & Narayan (2005) followed Brown (2000) and assumed the energy generated by electron captures, neutron emissions, and pycnonuclear reactions in the crust was distributed uniformly between $\Sigma_{12} = 6\times10^3$ and 2×10^5. We now follow Haensel & Zdunik (2008) and distribute the energy according to their Table A.3. (2) Plasma screening reduces the entrance channel width $\Gamma_{\rm C}$. Therefore, the plasma screening enhancement for the resonant contribution to the reaction rate includes a correction factor that reduces the overall enhancement (Salpeter & Van Horn 1969; Mitler 1977), although the reduction is only a few percent for the conditions relevant for superbursts (see, e.g., Fig. 1 of Cussons et al. 2002). We now use the formalism of Itoh et al. (2003) for the plasma enhancement factors of both the resonant and nonresonant contributions.

The ^{12}C + ^{12}C reaction rate, accretion rate $\dot\Sigma$, and ocean temperature profile together determine $\Sigma_{\rm ign}$. The temperature profile is a strong function of the crust's thermal conductivity and core's neutrino emissivity, both of which are

poorly constrained. We parametrize these uncertainties by implementing two conductivity and three core neutrino emissivity prescriptions that likely bracket their true values in accreting neutron stars. The thermal conductivity is a decreasing function of the impurity parameter $Q_{\rm imp} = \langle Z^2\rangle - \langle Z\rangle^2$ (Itoh & Kohyama 1993, see also Daligault & Gupta 2009). Schatz et al. (1999) found $Q_{\rm imp} \sim 100$ from steady-state nucleosynthesis calculations, although subsequent calculations suggest $Q_{\rm imp}$ should be smaller (Schatz et al. 2003a; Woosley et al. 2004a; Koike et al. 2004; Horowitz et al. 2007, 2009). In addition, fits to the quiescent light curves of KS 1731−260 (Shternin et al. 2007; Brown & Cumming 2009) and MXB 1659−29 (Brown & Cumming 2009) require that $Q_{\rm imp} \sim 1$. Since both observations and molecular dynamics simulations imply the crust forms an ordered lattice, we adopt $Q_{\rm imp}$ = 3 and 100 as the two bracketing values. The core neutrino emissivity, and thereby the core cooling rate, depends on the unknown ultradense matter equation of state (for reviews, see Yakovlev & Pethick 2004; Page et al. 2006). We consider one "fast" cooling model for which the pion condensate process dominates and two "slow" cooling models for which either the modified Urca or nucleon-nucleon bremsstrahlung process dominates (see, e.g., Table 1 of Page et al. 2006); these roughly correspond to cases "A," "B," and "D" of Cumming et al. (2006, see their Table 2). The respective core temperatures for these models are approximately 3×10^7 K, 3×10^8 K, and 6×10^8 K.

Figure 3 shows the superburst ignition column depth $\Sigma_{\rm ign}$ as a function of $\dot\Sigma/\dot\Sigma_{\rm Edd}$ for various neutron star models[5]. A 1.5 MeV resonance in the ^{12}C + ^{12}C system lowers $\Sigma_{\rm ign}$ by a factor ≈ 2 and ≈ 4 for the fiducial and maximum $(\omega\gamma)_{\rm R}$ values, respectively; the lowered $\Sigma_{\rm ign}$ values are in accord with the observationally inferred values for a range of realistic neutron star model parameters. Therefore, we conclude that (1) a strong resonance may exist at an energy ≈ 1.5 MeV above the ^{12}C + ^{12}C ground state, and (2) if such a resonance exists, it will mitigate the discrepancy between observationally inferred superburst ignition depths and those calculated from theoretical models.

For the low-mass X-ray transient 4U 1608−522, which exhibited a superburst, the thermal quiescent luminosity constrains the core temperature to be $\approx 2.5\times10^8$ K. Fits to the superburst light curve find an ignition column $\Sigma_{\rm ign} = (1.5\text{–}4.1)\times 10^{12}$ g cm^{-2}. A resonance at 1.5 MeV could make the ignition temperature over this range as low as $(4.1\text{–}4.8)\times10^8$ K, which is marginally consistent with the calculated crust temperature at the time of the superburst (Keek et al. 2007).

For the transient KS 1731−260, the timescale for the effective temperature to decrease implies $Q_{\rm imp} \lesssim 1$, and the lowest observed effective temperature implies that the core temperature is $\lesssim 10^8$ K (Shternin et al. 2007; Brown & Cumming 2009). Under these conditions, the temperature at $\Sigma \approx 10^{12}$ g cm^{-2} is unlikely to be $> 3\times10^8$ K and therefore too cold to match the inferred ignition depth, even if the proposed resonance exists. Recent theoretical calculations of nuclear reactions in the neutron star crust suggest that the pycnonuclear fusion of neutron-rich, low-Z ions such as ^{24}O (Horowitz et al. 2008) or reactions triggered by β-delayed neutron emissions (Gupta et al. 2008) may provide a strong source of heating for the neutron star outer crust. Indeed, fits to the quiescent light curves of KS 1731−260 and MXB 1659−29 suggest that the heating in the outer crust is larger than can be accounted for from electron captures (Brown & Cumming 2009). Although a survey of neutron star models with this additional heating is outside the scope of this paper, we note that a strong resonance does alleviate the discrepancy in $\Sigma_{\rm ign}$ even if it does not entirely resolve it.

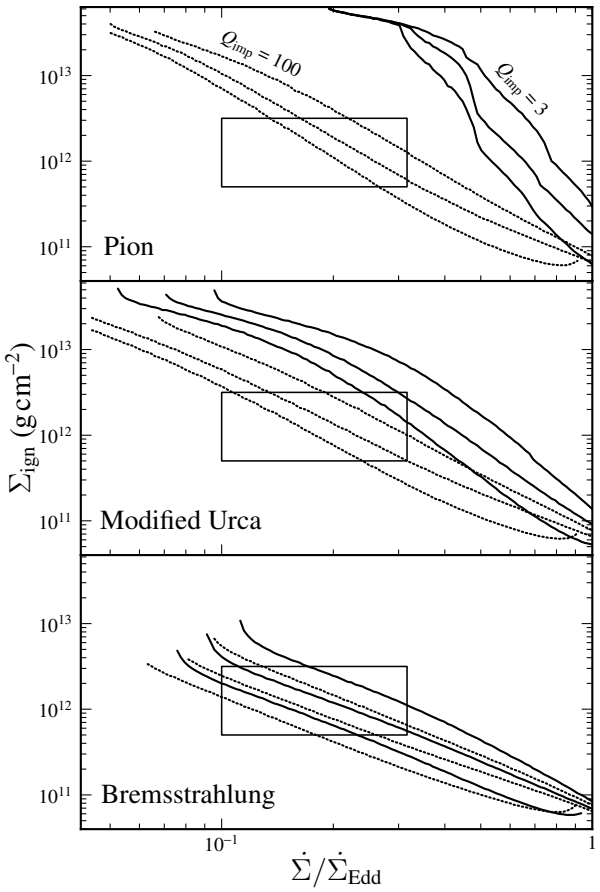

FIG. 3.— Superburst ignition column depth $\Sigma_{\rm ign}$ as a function of the Eddington-scaled accretion rate $\dot\Sigma/\dot\Sigma_{\rm Edd}$ for various model parameters. Solid (dashed) lines show results for models with impurity parameter $Q_{\rm imp}$ = 3 (100). "Pion," "Modified Urca," and "Bremsstrahlung" refer to the core's dominant neutrino emission mechanism. For a given $Q_{\rm imp}$ and neutrino emission mechanism, the three lines show results for a ^{12}C + ^{12}C reaction rate with no resonances (the standard rate), a hypothetical 1.5 MeV resonance with the fiducial strength $(\omega\gamma)_{\rm R} = 3.4\times10^{-8}$ eV, and a hypothetical 1.5 MeV resonance with an approximate maximum strength $(\omega\gamma)_{\rm R} = 3.4\times10^{-7}$ eV, from top to bottom. The boxes show the inferred $\Sigma_{\rm ign}$ and $\dot\Sigma$ ranges for the majority of observed superbursts. A 1.5 MeV resonance lowers $\Sigma_{\rm ign}$ by a factor ≈ 2 and ≈ 4 for the fiducial and maximum $(\omega\gamma)_{\rm R}$ values, respectively.

6. SUMMARY AND DISCUSSION

In this work, we reexamined the superburst trigger mechanism to address the discrepancy between observationally inferred superburst ignition column depths $\Sigma_{\rm ign}$ and those calculated in theoretical models. Motivated by the suggestion of Kuulkers et al. (2002b) and the similarity between inferred ignition column depths from different sources, we first ex-

[5] The critical $\dot\Sigma$ below which ^{12}C burns stably calculated in our global stability analysis is lower than that calculated in the one-zone model of Cumming et al. (2006, compare to their Fig. 15). The reason is simple: Following Cumming & Bildsten (2001), they demand that the characteristic lifetime of a ^{12}C ion $X_{\rm C}/r_{\rm nuc} > t_{\rm acc}$. However, $r_{\rm nuc}$ depends exponentially on the density due to plasma screening (§4.1), so ^{12}C burning occurs in a narrow column depth range, much like the electron captures discussed in §2.3. Thus, the proper criterion is $X_{\rm C}/r_{\rm nuc} > t_{\rm acc}\Delta\Sigma/\Sigma$, where $\Delta\Sigma/\Sigma$ is similar to the expression given in equation (10). This proper criterion gives a lower critical $\dot\Sigma$, in accord with our results.

plored the viability of thermally unstable electron captures as the trigger mechanism in §2. We found that electron captures are always thermally stable in accreting neutron star oceans; thus electron captures do not trigger superbursts. We then investigated the viability of nuclear fusion reactions other than ^{12}C + ^{12}C. Accretion-induced nuclear reactions deplete ions with $Z < 6$ at column depths $\Sigma \ll \Sigma_{\rm ign}$, whereas ions with $Z > 6$ fuse at $\Sigma \gg \Sigma_{\rm ign}$. We therefore confirmed the proposal (Cumming & Bildsten 2001; Strohmayer & Brown 2002) that ^{12}C + ^{12}C triggers superbursts.

We then examined the ^{12}C + ^{12}C fusion rate in §4, noting that superburst model results would be in accord with observations if the true fusion rate were greater than the standard rate by a factor $\gtrsim 10^2$. Two factors determine the fusion rate: plasma screening effects and the nuclear cross-section $\sigma(E)$. Uncertainties in, and corrections to, the plasma screening enhancement to the reaction rate alter the usual enhancement by a factor < 2 and thus cannot resolve the discrepancy between superburst observations and theoretical models. However, uncertainties in $\sigma(E)$ are much larger; indeed, $\sigma(E)$ is experimentally unknown at astrophysically relevant energies. We find that a strong resonance in the ^{12}C + ^{12}C system at an energy near 1.5 MeV could increase the fusion rate by a few orders of magnitude at the temperatures relevant to superbursts. Both theoretical optical potential models and extrapolations of existing experimental data suggest a resonance exists at an energy near 1.5 MeV. If this is true and the resonance strength $(\omega\gamma)_{\rm R}$ is sufficiently large, it could eliminate the discrepancy between observationally inferred superburst ignition column depths and theoretical model results (see Figure 3).

In §1 we outlined three fundamental problems that exist with superburst ignition. We address these problems below in the context of our results.

(1) The results of all previous superburst models imply that ocean temperatures are too low for ^{12}C ignition at the inferred $\Sigma_{\rm ign} \approx 10^{12}$ g cm^{-2}. A strong resonance near 1.5 MeV in the ^{12}C + ^{12}C system would decrease the temperature required for ignition at $\Sigma_{\rm ign} \approx 10^{12}$ g cm^{-2} from $\approx 6 \times 10^8$ K to $\approx 5 \times 10^8$ K.

(2) Heavy-ion fusion hindrance would imply that the standard S-factor overestimates the true ^{12}C + ^{12}C fusion rate. This existence of such hindrance is currently speculative for both ^{12}C + ^{12}C in particular (Jiang et al. 2007) and exothermic fusion reactions in general (Jiang et al. 2008; Stefanini et al. 2008). Furthermore, the effect heavy-ion fusion hindrance has on resonant reactions is unknown. Therefore, it is unclear whether heavy-ion fusion hindrance poses a problem for superburst ignition.

(3) The ^{12}C yield from nucleosynthesis models is often lower than that required for a thermal instability. A strong resonance would reduce the minimum ^{12}C abundance required for a superburst, but by only a small amount. Thus, this problem would be attenuated but not resolved.

Our result has implications for ^{12}C+^{12}C reactions in other contexts, namely Type Ia supernovae and massive stellar evolution. In addition, we have also presented a general prescription for understanding the screening enhancement factor in a multicomponent plasma. We briefly describe each of these topics before concluding with an outlook on future measurements.

6.1. *Implications for Type Ia Supernovae and Massive Stellar Evolution*

The fusion of ^{12}C is an important stage in the post–main-sequence evolution of a massive star, and it is the reaction that ignites a white dwarf and triggers a thermonuclear (Type Ia) supernova. In both systems, the competition between heating from the ^{12}C + ^{12}C reaction and cooling from neutrino emissions determines ignition. To explore the implications of a resonance in the reaction cross-section on these phenomena, we construct ignition curves (Fig. 4), defined as $\epsilon_{\rm nuc}(\rho, T) = \epsilon_\nu(\rho, T)$, for a ^{12}C-^{16}O plasma with $X_{\rm C} = 0.5$. We compute the neutrino emissivity for the pair, photo, plasma, and bremsstrahlung processes using analytical fitting formulae (Itoh et al. 1996). For $\epsilon_{\rm nuc}$, we use the effective reaction $\mathcal{Q}$-value of 9.0 MeV (Chamulak et al. 2008), which includes heating from both the p- and α- branches and subsequent reactions; the ignition curve is insensitive to the choice of $\mathcal{Q}$. Three curves are plotted in Fig. 4 for different choices of the ^{12}C + ^{12}C rate: the standard nonresonant rate (Caughlan & Fowler 1988, *dotted line*), a resonance at $E_{\rm R} = 1.5$ MeV with our fiducial strength $(\omega\gamma)_{\rm R} = 3.4 \times 10^{-8}$ eV (*solid line*), and a resonance at $E_{\rm R} = 1.5$ MeV with our maximum strength $(\omega\gamma)_{\rm R} = 3.4 \times 10^{-7}$ eV (*dashed line*).

As is evident from Figure 4, the effect of a resonance at $E_{\rm R} = 1.5$ MeV is minimal for the ignition of Type Ia supernovae, which are thought to ignite at central densities $> 10^9$ g cm^{-3} (see, e. g., Woosley et al. 2004b). It is interesting to speculate that a resonance at a lower energy might shift the ignition curve to lower densities. This would reduce the *in situ* neutronization of the nickel-peak material synthesized in the explosive burning and the neutronization during the pre-explosive convective burning (Piro & Bildsten 2008; Chamulak et al. 2008); moreover, numerical simulations (Röpke et al. 2006) find that a lower central density reduces the growth of the turbulent flame velocity (because the lower gravitational acceleration decreases the growth rate of the Rayleigh-Taylor instability), which leads to a less vigorous explosion and a decreased production of iron-peak elements. Although lower densities are necessary to avoid overproduction of neutron-rich isotopes such as ^{54}Fe and ^{58}Ni (Woosley 1997; Iwamoto et al. 1999), this may be ameliorated by improved electron capture rates onto pf-shell nuclei (Martínez-Pinedo et al. 2000; Brachwitz et al. 2000). Moreover, there is observational evidence that the majority of supernovae do undergo electron-captures in the innermost $\approx 0.2\ M_\odot$ of ejecta (Mazzali et al. 2007). Given the uncertainties in modeling the progenitor evolution, flame ignition, and explosion, and in the dependence of the ignition density on the accretion history of the white dwarf (see Lesaffre et al. 2006, for a recent discussion), we do not think it possible to constrain the existence of such a resonance from observations at this time, but future modeling efforts should clearly allow for this possibility.

Intriguingly, the largest effect is at $\rho \lesssim 10^5$ g cm^{-3}, which is the region encountered by post–main-sequence massive stars (see Woosley et al. 2002, and references therein). Stellar evolutionary calculations, which include the shock-induced explosive nucleosynthesis, find that a decrease in the ^{12}C + ^{12}C rate leads to enhancements in ^{26}Al and ^{60}Fe abundances (Gasques et al. 2007). Further calculations are needed to determine whether an enhanced ^{12}C + ^{12}C rate would produce interesting changes in nucleosynthesis.

6.2. *Ignition in a Multicomponent Plasma*

In §4.1.1 we showed that heavy spectator ions increase the plasma screening enhancement to the thermonuclear reaction

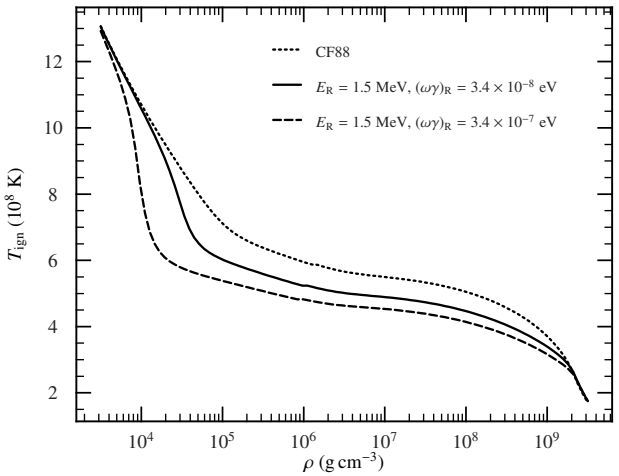

FIG. 4.— Locus in the temperature-density plane where $\epsilon_{nuc} = \epsilon_\nu$, which defines the ignition of ^{12}C for stellar burning in massive stars and for thermonuclear (Type Ia) supernovae. The composition is ^{12}C-^{16}O with $X_C = 0.5$. The three curves, from top to bottom, show ϵ_{nuc} computed with the standard rate (Caughlan & Fowler 1988, *dotted line*), with a resonance at our fiducial strength, $(\omega\gamma)_R = 3.4 \times 10^8$ eV (*solid line*), and with a resonance at our maximum strength, $(\omega\gamma)_R = 3.4 \times 10^{-7}$ eV (*dashed line*).

rate via linear mixing rule deviations. To our knowledge, this work is the first to show that spectator ions affect the plasma screening enhancement in the thermonuclear regime. Prior work on the effects such deviations have on the plasma screening enhancement focused on binary ionic mixtures consisting only of reactants and products (e.g. ^{12}C and ^{24}Mg) but no spectator ions (e.g. Ogata et al. 1993; DeWitt et al. 1996), and DeWitt & Slattery (2003) concluded that linear mixing rule deviations always decrease the plasma screening enhancement in binary ionic mixtures (eq. [36]). However, determining the effect of spectator ions requires analyzing a mixture of three or more ions, but previous applications of linear mixing rule deviations in ternary ionic mixtures (e. g., Ogata et al. 1993) focused only on phase diagrams of crystallizing white dwarfs (e. g., Isern et al. 1991; Segretain 1996), not on fusion reactions.

In our analysis, we tacitly assumed the plasma is uniformly mixed. However, recent molecular dynamics simulations of multicomponent plasmas exhibit clustering of low-Z ions (Wünsch et al. 2008; Horowitz et al. 2009), which may enhance the reaction rate. This is worthy of further investigation.

For completeness, we note that linear mixing rule deviations are much larger for Coulomb solids (DeWitt & Slattery 2003). This has two consequences for accreting neutron stars: (1) Screening enhancements for multicomponent plasmas in the pycnonuclear regime may be orders of magnitude greater than currently thought. This could lower the pressures at which pycnonuclear reactions occur in the crust and thereby heat the ocean to a larger extent. (2) A multicomponent plasma's freezing temperature is much lower than that of a one-component plasma. This possibly explains the results of Horowitz et al. (2007), whose molecular dynamics simulation of a multicomponent plasma froze at $\Gamma \approx 247$ rather than the typical $\Gamma \approx 175$ of a one-component plasma.

6.3. *Outlook for Future Measurements*

Our conclusions are contingent on the existence of a strong resonance near 1.5 MeV in the ^{12}C + ^{12}C system. As noted in §4.2, resonances exist throughout the experimentally studied energy range and are spaced at intervals of ≈ 0.3 MeV. Therefore, a resonance almost certainly exists sufficiently near 1.5 MeV (i.e., within the Gamow window). We cannot predict with confidence, however, that the resonance strength $(\omega\gamma)_R$ is sufficiently large. Indeed, the measured resonances at higher energies typically increase the thermally averaged reaction rate $\langle\sigma v\rangle$ by a factor $\lesssim 10$ over the nonresonant contribution, so the resonance needs to be unusually strong. Resolving this issue requires experimental measurements of the ^{12}C + ^{12}C cross-section near the Gamow peak, which requires lab energies of 3 MeV with the ability to measure cross-sections at the 0.1 pb level. Measurements at higher energies are probably required to map out the resonance structure between the Gamow peak and the other available measurements of the fusion cross-section. Such measurements are possible in the near term with existing laboratories and are certainly within reach of planned underground facilities such as DUSEL (though they will require the larger DUSEL accelerator option; Görres & Wiescher 2006).

We thank Lars Bildsten, Philip Chang, Andrey Chugunov, Richard Cyburt, Daniel Kasen, Hendrik Schatz, Michael Wiescher, Dima Yakovlev, Remco Zegers, and the anonymous referee for their advice and feedback. The Joint Institute for Nuclear Astrophysics (*JINA*) supported this work under NSF-PFC grant PHY 02-16783. AWS and EFB are supported by NASA/ATFP grant NNX08AG76G, and RLC is supported by the National Science Foundation under Grant No. NSF PHY05-51164.

APPENDIX

DERIVATION OF $\Delta H(0)$

In this Appendix, we derive $\Delta H(0)$, the correction to the plasma screening enhancement factor due to linear mixing rule deviations. Consider a strongly-coupled Coulomb plasma consisting of $N \equiv \sum_i N_i$ ions, where N_i is the number of ions with charge Z_i, $x_i \equiv N_i/N$ is the number fraction of species i, and species 1 and 2 are the reactant and product of the reaction, respectively, so that $Z_2 = 2Z_1$. DeWitt et al. (1973) found that, neglecting quantum contributions, $H(0)$ equals the difference in the Coulomb free energy before and after the reaction; since a fusion reaction destroys two reactant ions and creates one product ion,

$$H(0) = F^{\rm ex,initial} - F^{\rm ex,final} = F^{\rm ex}(N_1, N_2, ..., N_n) - F^{\rm ex}(N_1 - 2, N_2 + 1, ..., N_n). \quad \text{(A1)}$$

Writing equation (A1) in a more general form,

$$H(0) = -\frac{F^{\rm ex}(N_1 - 2\Delta N_2, N_2 + \Delta N_2, ..., N_n) - F^{\rm ex}(N_1, N_2, ..., N_n)}{\Delta N_2}, \quad \text{(A2)}$$

where ΔN_2 is the number of products created. In the limit $\Delta N_2 \ll N_1, N_2$, equation (A2) simplifies to

$$H(0) = -\left(\frac{\partial}{\partial N_2} - 2\frac{\partial}{\partial N_1}\right) F^{\rm ex}. \tag{A3}$$

Using the general expression for $F^{\rm ex}$ (eq. [34]), we find

$$\frac{H(0)}{k_{\rm B}T} = 2f^{\rm ex}(\Gamma_1) - f^{\rm ex}(\Gamma_2) + \{\Delta f^{\rm ex} - \mathcal{D}\Delta f^{\rm ex}\}, \tag{A4}$$

where the term $2f^{\rm ex}(\Gamma_1) - f^{\rm ex}(\Gamma_2)$ is the well-known result for a plasma obeying the linear mixing rule (e.g., Jancovici 1977), the bracketed term is $\Delta H(0)/k_{\rm B}T$, and we have defined the operator

$$\mathcal{D} \equiv N\left(\frac{\partial}{\partial N_2} - 2\frac{\partial}{\partial N_1}\right) = \frac{\partial}{\partial x_2} - 2\frac{\partial}{\partial x_1} + \sum_{i=1}^{n} x_i \frac{\partial}{\partial x_i}. \tag{A5}$$

Potekhin et al. (2009) derived an accurate, analytic fitting formula for $\Delta f^{\rm ex}$ (see their eq. [16]). Using their formula for an unpolarized electron background, which is appropriate for a strongly-coupled Coulomb liquid, $\Delta f^{\rm ex} = \Delta f^{\rm ex}\left(\Gamma, \langle Z\rangle, \langle Z^2\rangle, \langle Z^{5/2}\rangle\right)$, where $\Gamma = \sum_i x_i \Gamma_i$ and $\langle Z^k\rangle = \sum_i x_i Z_i^k$. From equations (A4) and (A5) of this work and equations (12), (14), and (16) of Potekhin et al. (2009), we find

$$\frac{\Delta H(0)}{k_{\rm B}T} = \Delta f^{\rm ex}\left\{1 - \left[\frac{\partial \ln \Delta f^{\rm ex}}{\partial \ln \Gamma}\mathcal{D}\ln\Gamma + \frac{\partial \ln \Delta f^{\rm ex}}{\partial \ln \langle Z\rangle}\mathcal{D}\ln\langle Z\rangle + \frac{\partial \ln \Delta f^{\rm ex}}{\partial \ln \langle Z^2\rangle}\mathcal{D}\ln\langle Z^2\rangle + \frac{\partial \ln \Delta f^{\rm ex}}{\partial \ln \langle Z^{5/2}\rangle}\mathcal{D}\ln\langle Z^{5/2}\rangle\right]\right\}, \tag{A6}$$

where

$$\begin{aligned}
&\frac{\partial \ln \Delta f^{\rm ex}}{\partial \ln \Gamma} = -\frac{abc\Gamma^b}{1+a\Gamma^b}, \qquad \mathcal{D}\ln\Gamma = 1 + (2^{5/3}-2)\frac{\Gamma_1}{\Gamma}, \qquad \mathcal{D}\ln\langle Z^k\rangle = 1 + (2^k-2)\frac{Z_1^k}{\langle Z^k\rangle}, \\
&\frac{\partial \ln \Delta f^{\rm ex}}{\partial \ln \langle Z\rangle} = -\frac{1}{2}\frac{\zeta^{\rm DH}}{\zeta^{\rm DH}-\zeta^{\rm LM}} - \frac{ac\Gamma^b}{1+a\Gamma^b}\left[\frac{1.1+34\delta^3}{2.2\delta+17\delta^4}(1-\delta) + 0.4b\left(\ln\Gamma + \frac{1}{1-b}\right)\right] + \frac{d}{3}\ln(1+a\Gamma^b), \\
&\frac{\partial \ln \Delta f^{\rm ex}}{\partial \ln \langle Z^2\rangle} = \frac{3}{2}\frac{\zeta^{\rm DH}}{\zeta^{\rm DH}-\zeta^{\rm LM}} + \frac{ac\Gamma^b}{1+a\Gamma^b}\left[\frac{3.3+102\delta^3}{2.2\delta+17\delta^4}(1-\delta) + 0.2b\left(\ln\Gamma + \frac{1}{1-b}\right)\right] - \frac{d}{6}\ln(1+a\Gamma^b), \\
&\frac{\partial \ln \Delta f^{\rm ex}}{\partial \ln \langle Z^{5/2}\rangle} = -\frac{\zeta^{\rm LM}}{\zeta^{\rm DH}-\zeta^{\rm LM}} - \frac{ac\Gamma^b}{1+a\Gamma^b}\left[\frac{2.2+68\delta^3}{2.2\delta+17\delta^4}(1-\delta)\right].
\end{aligned} \tag{A7}$$

REFERENCES

Aguilera, E. F., Rosales, P., Martinez-Quiroz, E., Murillo, G., Fernández, M., Berdejo, H., Lizcano, D., Gómez-Camacho, A., Policroniades, R., Varela, A., Moreno, E., Chávez, E., Ortíz, M. E., Huerta, A., Belyaeva, T., & Wiescher, M. 2006, Phys. Rev. C, 73, 064601

Alastuey, A. & Jancovici, B. 1978, ApJ, 226, 1034

Almqvist, E., Bromley, D. A., & Kuehner, J. A. 1960, Phys. Rev. Lett., 4, 515

Barrón-Palos, L., Aguilera, E. F., Aspiazu, J., Huerta, A., Martínez-Quiroz, E., Monroy, R., Moreno, E., Murillo, G., Ortiz, M. E., Policroniades, R., Varela, A., & Chávez, E. 2006, Nucl. Phys. A, 779, 318

Barrón-Palos, L., Chávez, E., Huerta, A., Ortiz, M. E., Murillo, G., Aguilera, E. F., Martínez-Quiroz, E., Moreno, E., Policroniades, R., & Varela, A. 2004, Rev. Mex. Fís., 50, 18

Becker, H. W., Kettner, K. U., Rolfs, C., & Trautvetter, H. P. 1981, Zeitschrift fur Physik, 303, 305

Betts, R. R. & Wuosmaa, A. H. 1997, Reports on Progress in Physics, 60, 819

Bildsten, L. 1998a, ApJ, 501, L89

Bildsten, L. 1998b, in The Many Faces of Neutron Stars, ed. R. Buccheri, J. van Paradijs, & M. A. Alpar (Dordrecht: Kluwer), 419

Bildsten, L. & Cumming, A. 1998, ApJ, 506, 842

Blaes, O., Blandford, R., Madau, P., & Koonin, S. 1990, ApJ, 363, 612

Blaschke, D., Sandin, F., Klähn, T., & Berdermann, J. 2008, in press (arXiv:0807.0414)

Brachwitz, F., Dean, D. J., Hix, W. R., Iwamoto, K., Langanke, K., Martínez-Pinedo, G., Nomoto, K., Strayer, M. R., Thielemann, F., & Umeda, H. 2000, ApJ, 536, 934

Bromley, D. A., Kuehner, J. A., & Almqvist, E. 1960, Phys. Rev. Lett., 4, 365

Brown, E. F. 2000, ApJ, 531, 988

—. 2004, ApJ, 614, L57

Brown, E. F. & Bildsten, L. 1998, ApJ, 496, 915

Brown, E. F. & Cumming, A. 2009, ApJ, 698, 1020

Cackett, E. M., Wijnands, R., Linares, M., Miller, J. M., Homan, J., & Lewin, W. H. G. 2006, MNRAS, 372, 479

Cackett, E. M., Wijnands, R., Miller, J. M., Brown, E. F., & Degenaar, N. 2008, ApJ, 687, L87

Cameron, A. G. W. 1959, ApJ, 130, 429

Caughlan, G. R. & Fowler, W. A. 1988, At. Data Nucl. Data Tables, 40, 283

Chabrier, G. & Ashcroft, N. W. 1990, Phys. Rev. A, 42, 2284

Chabrier, G. & Potekhin, A. Y. 1998, Phys. Rev. E, 58, 4941

Chamulak, D. A., Brown, E. F., Timmes, F. X., & Dupczak, K. 2008, ApJ, 677, 160

Chugunov, A. I., Dewitt, H. E., & Yakovlev, D. G. 2007, Phys. Rev. D, 76, 025028

Clayton, D. D. 1983, Principles of Stellar Evolution and Nucleosynthesis (Chicago: Univ. Chicago Press)

Cooper, R. L., Mukhopadhyay, B., Steeghs, D., & Narayan, R. 2006, ApJ, 642, 443

Cooper, R. L. & Narayan, R. 2005, ApJ, 629, 422

Cumming, A. 2003, ApJ, 595, 1077

—. 2005, Nucl. Phys. A, 758, 439

Cumming, A. & Bildsten, L. 2001, ApJ, 559, L127

Cumming, A. & Macbeth, J. 2004, ApJ, 603, L37

Cumming, A., Macbeth, J., in 't Zand, J. J. M., & Page, D. 2006, ApJ, 646, 429

Cussons, R., Langanke, K., & Liolios, T. 2002, European Physical Journal A, 15, 291

Daligault, J. & Gupta, S. 2009, in press (arXiv:0905.0027)

Dasmahapatra, B., Čujec, B., & Lahlou, F. 1982, Nucl. Phys. A, 384, 257

DeWitt, H. E., Graboske, H. C., & Cooper, M. S. 1973, ApJ, 181, 439

DeWitt, H. E. & Slattery, W. 2003, Contrib. Plasma Phys., 43, 279

DeWitt, H. E., Slattery, W., & Chabrier, G. 1996, Physica B Condensed Matter, 228, 21

Endt, P. M. 1990, Nucl. Phys. A, 521, 1
Erb, K. A., Betts, R. R., Korotky, S. K., Hindi, M. M., Tung, P. P., Sachs, M. W., Willett, S. J., & Bromley, D. A. 1980, Phys. Rev. C, 22, 507
Firestone, R. B. 2007, Nuclear Data Sheets, 108, 2319
Fisker, J. L., Brown, E. F., Liebendörfer, M., Thielemann, F.-K., & Wiescher, M. 2005, Nucl. Phys. A, 752, 604
Fisker, J. L., Görres, J., Wiescher, M., & Davids, B. 2006, ApJ, 650, 332
Fisker, J. L., Schatz, H., & Thielemann, F.-K. 2008, ApJS, 174, 261
Fowler, W. A. & Hoyle, F. 1964, ApJS, 9, 201
Fujimoto, M. Y., Hanawa, T., & Miyaji, S. 1981, ApJ, 247, 267
Fuller, G. M., Fowler, W. A., & Newman, M. J. 1980, ApJS, 42, 447
—. 1985, ApJ, 293, 1
Fushiki, I. & Lamb, D. Q. 1987, ApJ, 317, 368
Galloway, D. K., Muno, M. P., Hartman, J. M., Psaltis, D., & Chakrabarty, D. 2008, ApJS, 179, 360
Galster, W., Treu, W., Dück, P., Fröhlich, H., & Voit, H. 1977, Phys. Rev. C, 15, 950
Gasques, L. R., Afanasjev, A. V., Aguilera, E. F., Beard, M., Chamon, L. C., Ring, P., Wiescher, M., & Yakovlev, D. G. 2005, Phys. Rev. C, 72, 025806
Gasques, L. R., Brown, E. F., Chieffi, A., Jiang, C. L., Limongi, M., Rolfs, C., Wiescher, M., & Yakovlev, D. G. 2007, Phys. Rev. C, 76, 035802
Görres, J. & Wiescher, M. 2006, "ALNA - Accelerator Laboratory for Nuclear Astrophysics Underground" obtained from http://www.deepscience.org
Gupta, S., Brown, E. F., Schatz, H., Möller, P., & Kratz, K. 2007, ApJ, 662, 1188
Gupta, S. S., Kawano, T., & Möller, P. 2008, Phys. Rev. Lett., 101, 231101
Haensel, P., Potekhin, A. Y., & Yakovlev, D. G. 2007, Neutron Stars 1: Equation of State and Structure (New York: Springer)
Haensel, P. & Zdunik, J. L. 1990, A&A, 227, 431
—. 2003, A&A, 404, L33
—. 2008, A&A, 480, 459
Hansen, J.-P., Torrie, G. M., & Vieillefosse, P. 1977, Phys. Rev. A, 16, 2153
Hansen, J.-P. & Vieillefosse, P. 1976, Phys. Rev. Lett., 37, 391
High, M. D. & Čujec, B. 1977, Nucl. Phys. A, 282, 181
Horowitz, C. J. & Berry, D. K. 2009, in press (arXiv:0904.4076)
Horowitz, C. J., Berry, D. K., & Brown, E. F. 2007, Phys. Rev. E, 75, 066101
Horowitz, C. J., Caballero, O. L., & Berry, D. K. 2009, Phys. Rev. E, 79, 026103
Horowitz, C. J., Dussan, H., & Berry, D. K. 2008, Phys. Rev. C, 77, 045807
Ichimaru, S. 1993, Reviews of Modern Physics, 65, 255
in 't Zand, J. J. M., Kuulkers, E., Verbunt, F., Heise, J., & Cornelisse, R. 2003, A&A, 411, L487
in't Zand, J. J. M., Cornelisse, R., & Cumming, A. 2004, A&A, 426, 257
Isern, J., Hernanz, M., Mochkovitch, R., & Garcia-Berro, E. 1991, A&A, 241, L29
Itoh, N., Hayashi, H., Nishikawa, A., & Kohyama, Y. 1996, ApJS, 102, 411
Itoh, N. & Kohyama, Y. 1993, ApJ, 404, 268
Itoh, N., Mitake, S., Iyetomi, H., & Ichimaru, S. 1983, ApJ, 273, 774
Itoh, N., Tomizawa, N., Wanajo, S., & Nozawa, S. 2003, ApJ, 586, 1436
Iwamoto, K., Brachwitz, F., Nomoto, K., Kishimoto, N., Umeda, H., Hix, W. R., & Thielemann, F. 1999, ApJS, 125, 439
Jancovici, B. 1977, Journal of Statistical Physics, 17, 357
Jiang, C. L., Back, B. B., Esbensen, H., Greene, J. P., Janssens, R. V. F., Henderson, D. J., Lee, H. Y., Lister, C. J., Notani, M., Pardo, R. C., Patel, N., Rehm, K. E., Seweryniak, D., Shumard, B., Wang, X., Zhu, S., Mişicu, S., Collon, P., & Tang, X. D. 2008, Phys. Rev. C, 78, 017601
Jiang, C. L., Esbensen, H., Rehm, K. E., Back, B. B., Janssens, R. V., Caggiano, J. A., Collon, P., Greene, J., Heinz, A. M., Henderson, D. J., Nishinaka, I., Pennington, T. O., & Seweryniak, D. 2002, Phys. Rev. Lett., 89, 052701
Jiang, C. L., Rehm, K. E., Back, B. B., & Janssens, R. V. F. 2007, Phys. Rev. C, 75, 015803
Joss, P. C. 1978, ApJ, 225, L123
Keek, L., in 't Zand, J. J. M., Kuulkers, E., Cumming, A., Brown, E. F., & Suzuki, M. 2007, A&A, submitted
Keek, L., in't Zand, J. J. M., & Cumming, A. 2006, A&A, 455, 1031
Keek, L., in't Zand, J. J. M., Kuulkers, E., Cumming, A., Brown, E. F., & Suzuki, M. 2008, A&A, 479, 177
Keek, L., Langer, N., & in 't Zand, J. J. M. 2009, A&A, in press (arXiv:0905.4477)
Kettner, K. U., Lorenz-Wirzba, H., & Rolfs, C. 1980, Zeitschrift fur Physik, 298, 65
Kettner, K. U., Lorenz-Wirzba, H., Rolfs, C., & Winkler, H. 1977, Phys. Rev. Lett., 38, 337
Koike, O., Hashimoto, M., Arai, K., & Wanajo, S. 1999, A&A, 342, 464
Koike, O., Hashimoto, M., Kuromizu, R., & Fujimoto, S. 2004, ApJ, 603, 242
Korotky, S. K., Erb, K. A., Willett, S. J., & Bromley, D. A. 1979, Phys. Rev. C, 20, 1014
Kuulkers, E. 2004, Nucl. Phys. B (Proc. Suppl.), 132, 466
—. 2005, The Astronomer's Telegram, 483, 1
Kuulkers, E., Homan, J., van der Klis, M., Lewin, W. H. G., & Méndez, M. 2002a, A&A, 382, 947
Kuulkers, E., in 't Zand, J. J. M., van Kerkwijk, M. H., Cornelisse, R., Smith, D. A., Heise, J., Bazzano, A., Cocchi, M., Natalucci, L., & Ubertini, P. 2002b, A&A, 382, 503
Langanke, K. & Martínez-Pinedo, G. 2001, At. Data Nucl. Data Tables, 79, 1
Lesaffre, P., Han, Z., Tout, C. A., Podsiadlowski, P., & Martin, R. G. 2006, MNRAS, 368, 187
Martínez-Pinedo, G., Langanke, K., & Dean, D. J. 2000, ApJS, 126, 493
Mazarakis, M. G. & Stephens, W. E. 1972, ApJ, 171, L97
—. 1973, Phys. Rev. C, 7, 1280
Mazzali, P. A., Röpke, F. K., Benetti, S., & Hillebrandt, W. 2007, Science, 315, 825
Michaud, G. J. & Vogt, E. W. 1972, Phys. Rev. C, 5, 350
Mitler, H. E. 1977, ApJ, 212, 513
Ogata, S. 1997, ApJ, 481, 883
Ogata, S., Iyetomi, H., & Ichimaru, S. 1991, ApJ, 372, 259
Ogata, S., Iyetomi, H., Ichimaru, S., & Van Horn, H. M. 1993, Phys. Rev. E, 48, 1344
Paczyński, B. 1983, ApJ, 264, 282
Page, D. & Cumming, A. 2005, ApJ, 635, L157
Page, D., Geppert, U., & Weber, F. 2006, Nucl. Phys. A, 777, 497
Parikh, A., José, J., Moreno, F., & Iliadis, C. 2008, ApJS, 178, 110
Patterson, J. R., Winkler, H., & Zaidins, C. S. 1969, ApJ, 157, 367
Peng, F., Brown, E. F., & Truran, J. W. 2007, ApJ, 654, 1022
Perez-Torres, R., Belyaeva, T. L., & Aguilera, E. F. 2006, Physics of Atomic Nuclei, 69, 1372
Piro, A. L. & Bildsten, L. 2007, ApJ, 663, 1252
—. 2008, ApJ, 673, 1009
Potekhin, A. Y., Baiko, D. A., Haensel, P., & Yakovlev, D. G. 1999, A&A, 346, 345
Potekhin, A. Y. & Chabrier, G. 2000, Phys. Rev. E, 62, 8554
Potekhin, A. Y., Chabrier, G., & Rogers, F. J. 2009, Phys. Rev. E, 79, 016411
Remillard, R., Morgan, E., & The ASM Team at MIT, N. 2005, The Astronomer's Telegram, 482, 1
Röpke, F. K., Gieseler, M., Reinecke, M., Travaglio, C., & Hillebrandt, W. 2006, A&A, 453, 203
Rosales, P., Aguilera, E. F., Martinez-Quiroz, E., Murillo, G., Policroniades, R., Varela, A., Moreno, E., Fernández, M., Berdejo, H., Aspiazu, J., Lizcano, D., García-Martínez, H., Gómez-Camacho, A., Chávez, E., Ortíz, M. E., Huerta, A., & Macías, R. 2003, Rev. Mex. Fís., 49, 88
Rosenfeld, Y. 1995, Phys. Rev. E, 52, 3292
—. 1996, Phys. Rev. E, 54, 2827
Rutledge, R. E., Bildsten, L., Brown, E. F., Pavlov, G. G., Zavlin, V. E., & Ushomirsky, G. 2002, ApJ, 580, 413
Sahrling, M. & Chabrier, G. 1998, ApJ, 493, 879
Salpeter, E. E. 1954, Australian Journal of Physics, 7, 373
Salpeter, E. E. & Van Horn, H. M. 1969, ApJ, 155, 183
Satkowiak, L. J., Deyoung, P. A., Kolata, J. J., & Xapsos, M. A. 1982, Phys. Rev. C, 26, 2027
Sato, K. 1979, Prog. Theor. Physics, 62, 957
Schatz, H., Aprahamian, A., Barnard, V., Bildsten, L., Cumming, A., Ouellette, M., Rauscher, T., Thielemann, F.-K., & Wiescher, M. 2001, Phys. Rev. Lett., 86, 3471
Schatz, H., Bildsten, L., & Cumming, A. 2003a, ApJ, 583, L87
Schatz, H., Bildsten, L., Cumming, A., & Ouellette, M. 2003b, Nucl. Phys. A, 718, 247
Schatz, H., Bildsten, L., Cumming, A., & Wiescher, M. 1999, ApJ, 524, 1014
Segretain, L. 1996, A&A, 310, 485
Shapiro, S. L. & Teukolsky, S. A. 1983, Black Holes, White Dwarfs, and Neutron Stars (New York: John Wiley & Sons, Inc.)
Shternin, P. S., Yakovlev, D. G., Haensel, P., & Potekhin, A. Y. 2007, MNRAS, 382, L43
Spillane, T., Raiola, F., Rolfs, C., Schürmann, D., Strieder, F., Zeng, S., Becker, H.-W., Bordeanu, C., Gialanella, L., Romano, M., & Schweitzer, J. 2007, Phys. Rev. Lett., 98, 122501
Spinka, H. & Winkler, H. 1974, Nucl. Phys. A, 233, 456
Stefanini, A. M., Montagnoli, G., Silvestri, R., Beghini, S., Corradi, L., Courtin, S., Fioretto, E., Guiot, B., Haas, F., Lebhertz, D., Mărginean, N., Mason, P., Scarlassara, F., Sagaidak, R. N., & Szilner, S. 2008, Phys. Rev. C, 78, 044607
Strohmayer, T. E. & Bildsten, L. 2006, in Compact Stellar X-Ray Sources, ed. W. H. G. Lewin and M. van der Klis (Cambridge: Cambridge Univ. Press), 113

Strohmayer, T. E. & Brown, E. F. 2002, ApJ, 566, 1045
Taam, R. E. & Picklum, R. E. 1978, ApJ, 224, 210
Treu, W., Fröhlich, H., Galster, W., Dück, P., & Voit, H. 1980, Phys. Rev. C, 22, 2462
Ushomirsky, G., Cutler, C., & Bildsten, L. 2000, MNRAS, 319, 902
Widom, B. 1963, J. Chem. Phys., 39, 2808
Wijnands, R., Guainazzi, M., van der Klis, M., & Méndez, M. 2002, ApJ, 573, L45
Woosley, S. E. 1997, ApJ, 476, 801
Woosley, S. E., Heger, A., Cumming, A., Hoffman, R. D., Pruet, J., Rauscher, T., Fisker, J. L., Schatz, H., Brown, B. A., & Wiescher, M. 2004a, ApJS, 151, 75
Woosley, S. E., Heger, A., & Weaver, T. A. 2002, Rev. Mod. Phys., 74, 1015
Woosley, S. E. & Taam, R. E. 1976, Nature, 263, 101
Woosley, S. E., Wunsch, S., & Kuhlen, M. 2004b, ApJ, 607, 921
Wünsch, K., Hilse, P., Schlanges, M., & Gericke, D. O. 2008, Phys. Rev. E, 77, 056404
Yakovlev, D. G., Gasques, L. R., Afanasjev, A. V., Beard, M., & Wiescher, M. 2006, Phys. Rev. C, 74, 035803
Yakovlev, D. G. & Pethick, C. J. 2004, ARA&A, 42, 169
Yakovlev, D. G. & Urpin, V. A. 1980, Soviet Ast., 24, 303